Expert Systems With Applications 116 (2019) 96–107

Contents lists available at ScienceDirect

Expert Systems With Applications

journal homepage: www.elsevier.com/locate/eswa

Enhancement of robustness of face recognition system through reduced gaussianity in Log-ICA

Mrinal Kanti Bhowmik[a,*], Priya Saha[a], Anu Singha[a], Debotosh Bhattacharjee[b], Paramartha Dutta[c]

[a] Department of Computer Science & Engineering, Tripura University (A Central University), Suryamaninagar, Tripura 799022, India
[b] Department of Computer Science and Engineering, Jadavpur University, Kolkata 700032, India
[c] Department of Computer and System Sciences, Visva-Bharati University, Santiniketan, West Bengal 731235, India

ARTICLE INFO

Article history:
Received 13 January 2018
Revised 4 August 2018
Accepted 28 August 2018
Available online 29 August 2018

Keywords:
Gaussianity
Log-ICA
Log-normal distribution
Noisy face image
Overlapping probability densities

ABSTRACT

By reducing the gaussianity, Independent Component Analysis (ICA) behaves robustly in segregating individual signals of non-skewed characteristic from a mixed composite signal. In this article, we present a next-generation variant of ICA, especially applicable in the skewed composite signal scenario, applying the Logarithmic transformation on basic ICA, named as Log-ICA. This approach is capable of decreasing overlapping probability densities of the composite signal, which, in turn, extracts more independent components because of reduced gaussianity. Here also we use two different architectures Log-ICA I and Log-ICA II corresponding to two variants of ICA architecture (ICA I and ICA II). We justify the effectiveness of the proposed technique on five separate benchmark face datasets using five classifiers. Out of five face datasets, two datasets contain both visible and thermal face images. Experimental results show that Log-ICA II performs better than Log-ICA I and two variants of ICA for original face images and noise-induced face images.

1. Introduction

The face recognition system has excellent potential in multimedia applications, e.g., human-machine interaction (Han, Otto, Liu, & Jain, 2015), online social networks (Choi, Neve, Plataniotis, & Ro, 2011; Ding & Tao, 2015), and digital entertainment. Face images in multimedia applications exhibit variations in pose (Yin & Liu, 2018), expression (Hsieh, Lai, & Chen, 2009; Zen, Porzi, Sangineto, Ricci, & Sebe, 2016), and illumination (Beveridge et al., 2015). In this paper, we are considering face recognition under all three variations using our proposed method named logarithmic ICA or Log-ICA.

The goal of ICA is to decompose the input dataset into a set of statistically independent components or as separate as possible. ICA can isolate data from mixed sources by maximizing their non-gaussianity. Non-gaussianity empowers the separation and identification of original components from the mixed source. Perfect Gaussian sources cannot be separated by ICA. Previously, Bartlett (Bartlett, Movellan, & Sejnowski, 2002) developed two ICA architectures for face recognition (ICA architecture I and ICA architecture II). The purpose of ICA architecture-I is to find statistically independent basis images, and ICA architecture-II is for finding factorial face code. Liu (Liu, 2004) proposed an enhanced ICA (EICA) method. EICA is computed in a reduced PCA space, and the dimension of the PCA space is computed by balancing the energy and magnitude criterion for enhanced retrieval performance. The proposed EICA method is experimented for content-based face image retrieval using the FERET database. Bartlett et al. (2002) implemented the infomax algorithm using a neural network approximation, while EICA applied a statistical algorithm (Liu, 2004) by decomposing it into three significant steps (whitening, rotations, and normalization). To reduce the effect of the dimensionality problem in ICA, Zhang, Gao, and Zhang (2007) proposed a block ICA (BICA) method. In BICA, the whole image is partitioned into equal size blocks, and a common demixing matrix for all the blocks is calculated. Experiment results suggest that BICA is computationally more efficient than ICA and it achieves higher recognition accuracy than ICA. In two of our earlier works (Bhowmik, Bhattacharjee, Basu, & Nasipuri, 2012, 2011), we use the concept of Log-ICA in one or other form for two specific purposes, dark image analysis and expression analysis for the respective small subset of IRIS (DOE University Research Program in Robotics, 2005) visual and thermal face dataset.

* Corresponding author.
E-mail addresses: mrinalkantibhowmik@tripurauniv.in (M.K. Bhowmik), debotosh@ieee.org (D. Bhattacharjee), paramartha@ieee.org (P. Dutta).

https://doi.org/10.1016/j.eswa.2018.08.047
0957-4174/

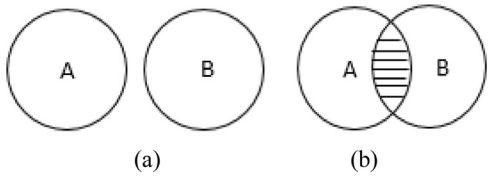

Fig. 1. (a) A and B are independent of each other; (b) A and B are partially overlapped to each other.

In this paper, we propose logarithmic ICA or Log-ICA, which can enhance the property of non-gaussianity to achieve better independent component separation for face image datasets through logarithmic transformation. Log-ICA tends the data towards non-gaussianity by reducing overlapping area formed by their respective probability densities. Therefore, the data obtained follow log-normal distribution and hence become skewed for our experimental datasets. In this work, we use face images available in the visual and thermal domains and also obtain the fused face images from those visual and thermal face images. The proposed system is also tested for visual face images under three different types of noisy situations namely additive, multiplicative, and impulse and found to be robust against all the three noises.

The paper contributes in five ways.

- A new variant of ICA, i.e., Log-ICA is proposed to increase non-gaussianity which is the basic principle for separation of independent components in ICA.
- Applying logarithmic transformation, the overlapping area of probability densities is reduced.
- Handling of difficult multiplicative noise becomes easier because multiplicative noise is converted into simpler additive noise due to logarithmic transformation.
- Facial expression may be considered as one type of multiplicative noise, and it is observed that the present method is capable of performing better in recognizing various expressions in comparison to the basic ICA.
- To establish the superiority of Log-ICA over other variants of ICA, several experiments are conducted for face and expression recognition. Depending on the availability of face images in the existing datasets, experiments are carried out on visual, thermal, and fused images with or without facial expressions. The same set of experiments is repeated under the three noisy situations.

The rest of the paper is as follows. Section 2 depicts the justification of logarithmic transformation and the Log-ICA. Section 3 illustrates the system overview of the proposed approach. Section 4 reports and discusses experiment results on benchmark databases. Finally, the conclusion is drawn in section 5.

2. Natural logarithm based ICA algorithm (Log-ICA)

According to the Central Limit Theorem (CLT), the definition of ICA says that the distribution of the sum of independent components tends toward a Gaussian or Normal distribution (Stone 2004Stone, 2004). The independent components can be extracted from a Gaussian mixture by making their linear transformation as non-gaussian as possible. For making the distribution of samples towards non-gaussianity, we propose Log-ICA which is based on the logarithmic transformation.

In this method, the independence property of individual components present in a mixture is increased to achieve higher separability. Suppose, A and B are two completely independent random events.

In the Venn diagram of Fig. 1(a), events A and B are disjoint. These events cannot both occur, so there is no overlapping area. In the Venn diagram of Fig. 1(b), we want to show that two random events A and B are not disjoint. This means that it is possible for both events to occur, and the overlapping area represents this possibility.

The idea of the overlapped area may work on following issues.

- In this paper, we consider the distribution of a large set of face images as Gaussian.
- The face images of different persons with different variations of a dataset may have an equal mean, but their variances may not be same because different class images (say, expression variations) have different orientations of pixel variations.
- Here, the areas of two Log-Normal curves are denoted by $A_{LN}{}^{(1)}$ and $A_{LN}{}^{(2)}$ respectively. Likewise, the areas of two Normal curves are indicated by $A_N{}^{(1)}$ and $A_N{}^{(2)}$ respectively. We have to prove that $A_{LN}{}^{(1)} \cap A_{LN}{}^{(2)} < A_N{}^{(1)} \cap A_N{}^{(2)}$.
- For a particular application, i.e., classification of face images with a different pose, illumination, expression variations, the proposition holds true.

Proposition. *The overlapping area of two* Log-*Normal curves in comparison to Normal curves is less if the variability of data increases.*

Proof. The overlapped area of the normal domain is denoted by λ_N $(A_N{}^{(1)} \cap A_N{}^{(2)})$ and the same for the log-normal domain is denoted by $\lambda_{LN}(A_{LN}{}^{(1)} \cap A_{LN}{}^{(2)})$. We prove that the overlapped area of log-normal curves is less than the overlapped area of normal curves, i.e. $\lambda_{LN} < \lambda_N$.

The Fig. 2(a) shows two normally distributed curves with mean μ and standard deviation $\sigma_1$and $\sigma_2$for a random variable$x$. In a normal distribution, the two curves intersect each other at a point P and Q. We can write

$$\frac{1}{\sqrt{2\pi}\sigma_1}\mathbf{exp}\left[-\frac{(x-\mu)^2}{2{\sigma_1}^2}\right] = \frac{1}{\sqrt{2\pi}\sigma_2}\mathbf{exp}\left[-\frac{(x-\mu)^2}{2{\sigma_2}^2}\right]$$

$$\Rightarrow \mathbf{exp}\left[-\frac{(x-\mu)^2}{2{\sigma_1}^2}+\frac{(x-\mu)^2}{2{\sigma_2}^2}\right] = \frac{\sigma_1}{\sigma_2}$$

$$\Rightarrow \frac{(x-\mu)^2}{2}\left[\frac{1}{{\sigma_2}^2}-\frac{1}{{\sigma_1}^2}\right] = \mathbf{log}\left(\frac{\sigma_1}{\sigma_2}\right)$$

$$\Rightarrow (x-\mu)^2 = 2\left(\frac{{\sigma_1}^2{\sigma_2}^2}{{\sigma_1}^2-{\sigma_2}^2}\right)\mathbf{log}\left(\frac{\sigma_1}{\sigma_2}\right)$$

$$\Rightarrow (x-\mu) = \pm\sqrt{\left(\frac{{\sigma_1}^2{\sigma_2}^2}{{\sigma_1}^2-{\sigma_2}^2}\right)\mathbf{log}\left(\frac{{\sigma_1}^2}{{\sigma_2}^2}\right)}$$

$$\Rightarrow x = \mu \pm \sqrt{\left(\frac{{\sigma_1}^2{\sigma_2}^2}{{\sigma_1}^2-{\sigma_2}^2}\right)\mathbf{log}\left(\frac{{\sigma_1}^2}{{\sigma_2}^2}\right)}$$

$$\Rightarrow x = \mu \pm k(\sigma_1,\sigma_2) \quad (1)$$

Let, $\frac{x-\mu}{\sigma_2} = t$

$\Rightarrow x-\mu = t\sigma_2$

$\Rightarrow x = \mu + t\sigma_2,$

$\Rightarrow dx = \sigma_2 dt$

$\frac{t}{\sqrt{2}} = p$

$dt = dp$

The percentage of overlapped area λ_N

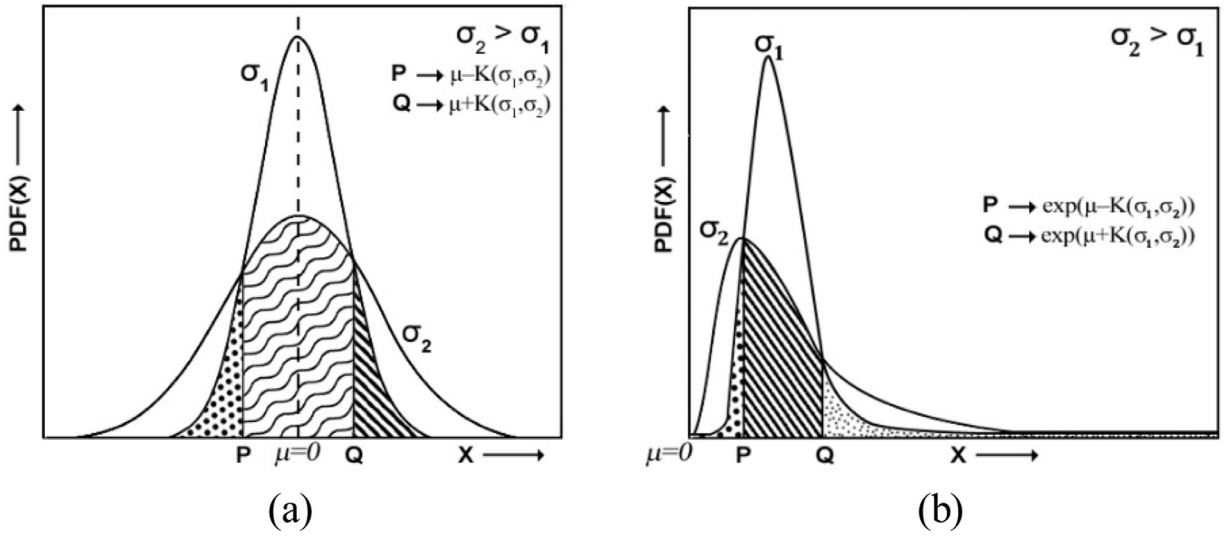

Fig. 2. (a) Normally distributed curves; (b) Log-normally distributed curves.

$$= \text{Area under } (\mu, \sigma_2) \text{ curve over } [\mu - k(\sigma_1, \sigma_2), \mu + k(\sigma_1, \sigma_2)]$$

$$= \frac{1}{\sqrt{2\pi\sigma_2^2}} \int_{\mu-k(\sigma_1,\sigma_2)}^{\mu+k(\sigma_1,\sigma_2)} \exp\left(-\frac{(x-\mu)^2}{2\sigma_2{}^2}\right) dx$$

$$= \frac{1}{\sqrt{2\pi\sigma_2^2}} \int_{\mu-k(\sigma_1,\sigma_2)}^{\mu+k(\sigma_1,\sigma_2)} \exp\left(-\frac{t^2}{2}\right) dt$$

$$= \frac{1}{\sqrt{2\pi\sigma_2^2}} \int_{\mu-k(\sigma_1,\sigma_2)}^{\mu+k(\sigma_1,\sigma_2)} \exp\left(-\frac{t^2}{2}\right) \sigma_2 dt$$

$$= \frac{1}{\sqrt{2\pi}} \int_{\mu-k(\sigma_1,\sigma_2)}^{\mu+k(\sigma_1,\sigma_2)} \exp\left(-\left(\frac{t}{\sqrt{2}}\right)^2\right) dt$$

$$= \frac{1}{\sqrt{2\pi}} \int_{\mu-k(\sigma_1,\sigma_2)}^{\mu+k(\sigma_1,\sigma_2)} \exp\left(-p^2\right) dp$$

$$= \frac{1}{\sqrt{2\pi}} \frac{\sqrt{\pi}}{2} [erf(p)]_{\mu-k(\sigma_1,\sigma_2)}^{\mu+k(\sigma_1,\sigma_2)}$$

$$= \frac{1}{2\sqrt{2}} (erf(\mu + k(\sigma_1, \sigma_2)) - erf(\mu - k(\sigma_1, \sigma_2))) \quad (2)$$

In Fig. 2(b), two curves intersect each other at point P and Q in a log-normal distribution.

$$\frac{1}{\sqrt{2\pi}x\sigma_1} \exp\left[-\frac{(\log x - \mu)^2}{2\sigma_1{}^2}\right] = \frac{1}{\sqrt{2\pi}x\sigma_2} \exp\left[-\frac{(\log x - \mu)^2}{2\sigma_2{}^2}\right]$$

$$\Rightarrow \exp\left[-\frac{(\log x - \mu)^2}{2\sigma_1{}^2} + \frac{(\log x - \mu)^2}{2\sigma_2{}^2}\right] = \frac{\sigma_1}{\sigma_2}$$

$$\Rightarrow \frac{(\log x - \mu)^2}{2} = \left(\frac{\sigma_1{}^2\sigma_2{}^2}{\sigma_1{}^2 - \sigma_2{}^2}\right) \times \log\left(\frac{\sigma_1}{\sigma_2}\right)$$

$$\Rightarrow (\log x - \mu)^2 = \left(\frac{\sigma_1{}^2\sigma_2{}^2}{\sigma_1{}^2 - \sigma_2{}^2}\right) \times \log\left(\frac{\sigma_1{}^2}{\sigma_2{}^2}\right)$$

$$\Rightarrow (\log x - \mu) = \pm\sqrt{\left(\frac{\sigma_1{}^2\sigma_2{}^2}{\sigma_1{}^2 - \sigma_2{}^2}\right) \log\left(\frac{\sigma_1{}^2}{\sigma_2{}^2}\right)}$$

$$\Rightarrow \log x = \mu \pm \sqrt{\left(\frac{\sigma_1{}^2\sigma_2{}^2}{\sigma_1{}^2 - \sigma_2{}^2}\right) \log\left(\frac{\sigma_1{}^2}{\sigma_2{}^2}\right)}$$

$$\Rightarrow x = \exp(\mu \pm k(\sigma_1, \sigma_2)) \quad (3)$$

Let, $\frac{\log x - \mu}{\sigma_2} = r$,

$\Rightarrow \log x = r\sigma_2 + \mu$,

$\Rightarrow \frac{1}{x} dx = dr\sigma_2$

$\Rightarrow dx = x\sigma_2 dr$

$\frac{r}{\sqrt{2}} = q$

$r = \sqrt{2}q$

$dr = dq$

The percentage of overlapped area λ_{LN}

$$= \text{Area under } (\mu, \sigma_2) \text{ curve over } [\mu - k(\sigma_1, \sigma_2), \mu + k(\sigma_1, \sigma_2)]$$

$$= \frac{1}{\sqrt{2\pi}x\sigma_2} \int_{\exp(\mu-k(\sigma_1,\sigma_2))}^{\exp(\mu+k(\sigma_1,\sigma_2))} \exp\left(-\frac{(\log x - \mu)^2}{2\sigma_2{}^2}\right) dx$$

$$= \frac{1}{\sqrt{2\pi}x\sigma_2} \int_{\exp(\mu-k(\sigma_1,\sigma_2))}^{\exp(\mu+k(\sigma_1,\sigma_2))} \exp\left(-\left(\frac{r}{\sqrt{2}}\right)^2\right) x\sigma_2 dr$$

$$= \frac{1}{\sqrt{2\pi}} \int_{\exp(\mu-k(\sigma_1,\sigma_2))}^{\exp(\mu+k(\sigma_1,\sigma_2))} \exp\left(-\left(\frac{r}{\sqrt{2}}\right)^2\right) dr$$

$$= \frac{1}{\sqrt{2\pi}} \int_{\exp(\mu-k(\sigma_1,\sigma_2))}^{\exp(\mu+k(\sigma_1,\sigma_2))} \exp\left(-q^2\right) dq$$

$$= \frac{1}{\sqrt{2\pi}} \frac{\sqrt{\pi}}{2} [erf(q)]_{\exp(\mu-k(\sigma_1,\sigma_2))}^{\exp(\mu+k(\sigma_1,\sigma_2))}$$

$$= \frac{1}{2\sqrt{2}} (erf(\exp(\mu + k9(\sigma_1, \sigma_2))) - erf(\exp(\mu - k(\sigma_1, \sigma_2)))) \quad (4)$$

According to the definition of error function *erf (x)* (Whittaker & Watson, 1990), the value of function is saturated i.e. it goes to 1

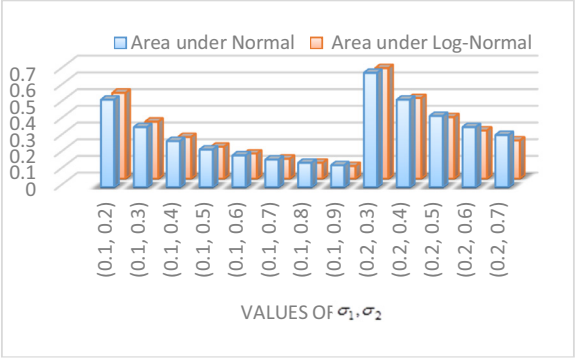

Fig. 3. A graphical plot of overlapped area in normal and log-normal distribution.

after certain degree of variability for any value of x and the value of $erf(\mu + k(\sigma_1,\sigma_2))$ will become smaller than $erf(\exp(\mu + k(\sigma_1,\sigma_2)))$.

Because of faster asymptotic convergence of exponential function compared to that of the linear counterpart, $(erf(\mu + k(\sigma_1,\sigma_2)) - erf(\mu - k(\sigma_1,\sigma_2))) > (erf(\exp(\mu + k(\sigma_1,\sigma_2))) - erf(\exp(\mu - k(\sigma_1,\sigma_2))))$.

Therefore, it can be concluded that the proposition holds true after a certain degree of variability of data. If there is no variation in data, then the technique is not applicable.

Hence, it is proved that $\lambda_{LN} < \lambda_N$.

We can also prove this by plotting a graph between the overlapped area and sample values of σ_1 and σ_2. The bar chart is given in Fig. 3.

It is noticed from Fig. 3 that the overlapped area of log-normal curves is less than the overlapped area of normal curves, i.e. $\lambda_{LN} < \lambda_N$. It is evident from the discussion that log-normal distribution helps to reduce the overlapped area (if any) between two random variables.

The effectiveness of log-normal distribution is also proved here by computing the error (E), given in (5), which is the sum of squares of the difference between relative frequency histogram and probability density function (pdf) of a particular distribution with estimated parameters.

$$E = \sum_{x} \left[h(x) - \hat{f}(x)_{p1\,p2} \right]^2, \tag{5}$$

where $h(x)$ is the relative frequency histogram, $\hat{f}(x)$ is the density estimation of a random variable and p_1, p_2 are the estimated parameters of the distribution. It is noticed in Fig. 4 that log-normal distribution generates less error than four other distributions namely Beta, Weibull, Gamma and Gaussian for the face datasets IRIS, FERET, CMU-PIE and USTC-NVIE except Yale database. Therefore, we use logarithmic transformation along with ICA to extract maximally independent components from a mixture of data samples and to increase classification accuracy.

3. Proposed system overview

Fig. 5 presents the block diagram of our proposed approach Log-ICA, which summarizes both architectures of ICA in the logarithm domain. In the pre-processing stage, the database face images are manually cropped, resized, and finally represented as a row or a column data matrix followed by Log-ICA architectures namely Log-ICA I and Log-ICA II. The proposed approach mainly consists of two pre-processing stages. The first pre-processing stage is log-centering that makes the distribution of data matrix to log-Normal. Then, PCA is used to project face patterns from a high-dimensional image space to low-dimensional space. The second

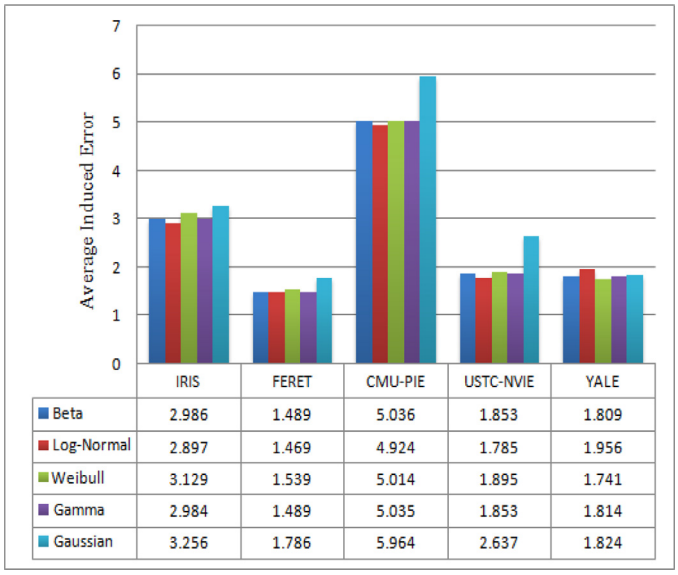

	IRIS	FERET	CMU-PIE	USTC-NVIE	YALE
Beta	2.986	1.489	5.036	1.853	1.809
Log-Normal	2.897	1.469	4.924	1.785	1.956
Weibull	3.129	1.539	5.014	1.895	1.741
Gamma	2.984	1.489	5.035	1.853	1.814
Gaussian	3.256	1.786	5.964	2.637	1.824

Fig. 4. Errors of different distributions.

pre-processing stage is log-whitening that changes the scales of variances instead of the unit variance. In the next stage, we invoke the ICA algorithm for maximizing non-gaussianity as a measure of statistical independence. The subspace obtained by ICA algorithm is used to project individual face images of the database, and projected images are considered as corresponding feature vectors. The optimality of the projection can be substantiated by the classification standpoint. In the next sub-section, we illustrate the details of Log-ICA.

3.1. Independent component analysis

Independent Component Analysis (ICA) is a generalization of PCA technique that assigns data from a high-dimensional space to a lower-dimensional space and decorrelates the higher-order statistics (Hyvarinen, 1999). ICA contains a set of basis vectors with maximum statistical independence whereas PCA deals with basis vectors which are orthogonal to each other but do not ensure statistical independence. ICA for face recognition operates within one of two different architectures, Architecture I and Architecture II.

ICA Architecture I presents the face images as a linear combination of a set of statistically independent basis images. To represent the image for use in recognition, ICA makes use of the reconstruction coefficients of a face image that are derived from these basis images. A given face dataset is organized into a data matrix, where each row vector is a different image. In this approach, images are random variables, and pixels are trials (Bartlett et al., 2002).

In ICA Architecture II, the face dataset is represented as a data matrix where each column vector is a face image. The main difference between these two architectures is that ICA Architecture I is talking about independence among face images, and ICA Architecture II tells about independence among face pixels. For simplicity, we use the terms ICA I and ICA II in place of ICA Architecture I and ICA Architecture II respectively.

Some popular ICA algorithms include FastICA (Bartlett et al., 2002; Hyvarinen, 1999), Infomax (Lee et al., 1999), Common's algorithm (Comon, 1994), and Kernel ICA (Bach & Jordan, 2002). In this paper, we use FastICA for implementation of ICA I, ICA II, Log-ICA I, and Log-ICA II.

The FastICA is based on a fixed-point iteration scheme (Belhumeur, Hespanha, & Kriegman, 1997) for finding the direction of the weight coefficient vector$\mathbf{W}$such that the projection $y = W^T X$

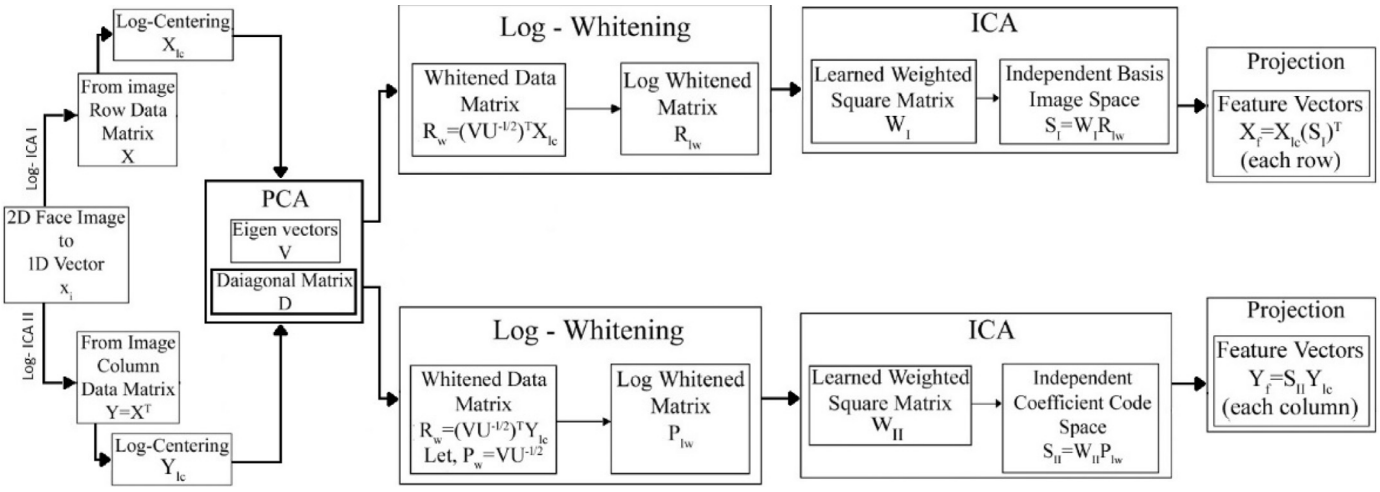

Fig. 5. Block diagram of Log-ICA.

maximizes non-gaussianity for the data matrixX. To computeW, the non-quadratic function (G) (Phillips, Martin, Wilson, & Przybocki, 2000) used here is given as

$$G(y) = -\exp\left(-\frac{y^2}{2}\right) \tag{6}$$

3.2. The proposed Log-ICA algorithm

We propose two versions of Log-ICA algorithm namely Log-ICA I and Log-ICA II based on two architectures of ICA. The whole algorithm is similar for Log-ICA I and log-ICA II except step 1 and step 2. Therefore, we present the detailed procedure of Log-ICA I algorithm.

Algorithm. Log-Independent Component Analysis (Log-ICA I)

Input: n number of 2D face images $x_i \in \Re^{p\times q}$for $i=1, 2, ..., n$; where p and q indicates the row and column numbers respectively. The number of desired components is d.
Output: Feature space S.
1. Convert each face image (x_i) as a vector of size $m=p\times q$.
2. Create a data matrix $X=[x_1,x_2,..., x_n]^T \in \Re^{n\times m}$.
3. (a) To make a zero-mean (zm) or center the data matrix X in a trial space $\Re^m$ by subtracting the mean column vector (μ) from each observation $\Re^n$ as:
$X_{zm} = \sum_{i=1}^{n}\sum_{j=1}^{m} x_{ij} - \frac{1}{m}\sum_{i=1}^{n} x_i = X - E(X) = X - \mu$
(b) Convert the zero-mean variables into the logarithmic domain, so the resulting log-centered (X_{lc}) is as follows:
$X_{lc}(i,j) = \frac{1}{\log(1+\max_value)} \log(1+abs(X_{zm}(i,j)))$max_$value$is the maximum value of X_{zm}.
4. In this step, whitened matrix (R_w) is computed as it is done in basic ICA and after that logarithmic transformation is taken to obtained log-whitening matrix (R_{lw})
(a) Calculate the orthonormal eigenvectors $V=[\alpha_1,\alpha_2,..., \alpha_d] \in \Re^{n\times d}$ of the covariance matrix $\sum = \frac{1}{m} X_{lc} X_{lc}^T$corresponding to the largest d positive eigenvalues $\lambda_1 \geq \lambda_2 \geq ... \geq \lambda_d$, and a matrix of its eigenvalues $U^{-1/2} = diag(\lambda_1^{-1/2}, \ldots, \lambda_d^{-1/2})$.
(b) Obtain the whitened data matrix as $R_w=(VU^{-1/2})^T X_{lc}$, $R_w \in \Re^{d\times m}$
(c) Convert the whitened variable into the logarithmic domain, so the resulting log-whitening data matrix (R_{lw}) is as follows:
$R_{lw}(i,j) = \frac{1}{\log(1+\max\_value)} \log(1+abs(R_w(i,j)))$
such that $E\{R_{lw}R_{lw}^T\} \cong D$ where D is a diagonal matrix.
5. Generate an unmixing square matrix $W \in \Re^{d\times d}$ and an independent basis image space $S=WR_{lw}$ through FastICA.

The algorithmic steps are described below.

The arrangement of face image (Steps 1–2): The conversion of each 2D face image (x_i) to 1D block reshapes a p-by-q matrix to a 1D vector with length $m=p\times q$. Then, a 2D data matrix X is created by combining all the converted 1D vectors as rows of X. However, in the case of ICA II, 1D image vectors are stored in the columns of the data matrix.

Transformation of centered data to the logarithmic domain, i.e., log-centered (Steps 3.a-3.b): The most basic and essential preprocessing is to center X, i.e., subtract its mean vector $\mu=E(X)$ to make Xa zero-mean variable.

This preprocessing is made solely to simplify the ICA algorithms. In this stage, the distribution of data matrix follows the standard Gaussian distribution according to Central Limit Theorem (CLT). In a practical scenario, the distribution of the data matrices is not gaussian somewhat arbitrary. In the case of ICA, the distribution should be non-gaussian and to ensure that, in this method, the logarithmic transformation is applied to the centered data, which is called log-centering of data.

Creation of Diagonal Matrix through the transformation of log-whitening (Steps 4.a–4.c): The second pre-processing approach of ICA is to whiten the observed variables such that its components are uncorrelated and their variances are equal to unity, i.e., the covariance matrix would be an identity matrix (Hyvärinen, Karhunen, & Oja, 2002). After whitening step, logarithmic transformation is applied to change the scales of variances instead of unit variance preserving the property of uncorrelation among the variables. However, the core motive of this log-whitening aids in increasing non-overlapping of density curves for the respective observed variables by differing variance values. The whitened covariance matrix (Fig. 6(b)) is exactly following the identity matrix by same diagonal values with yellow color cells, and rest of the cells contain values near to zero with purple color. The Fig. 6(c) is representing a covariance matrix of the log-whitening with the values of the diagonal cells of several colors which is an indication of a diagonal matrix. The values of the rest of the cells are almost zero except few of them.

Generation of independent subspace (Step 5): Subspace analysis techniques are widely used in face recognition (Bartlett et al., 2002; Liu, 2004; Zhang et al., 2007). Step 5 presents a subspace representation of face images which is learned through the FastICA algorithm for maximizing non-gaussianity as a measure of statistical independence.

3.3. Projection of face images

Any face image (x) given to the system for recognition goes through log-centering (x_{lc}) and then projected into the independent subspace S to obtain the feature vector (x^f), in (7).

$$x^f = x_{lc} S^T \tag{7}$$

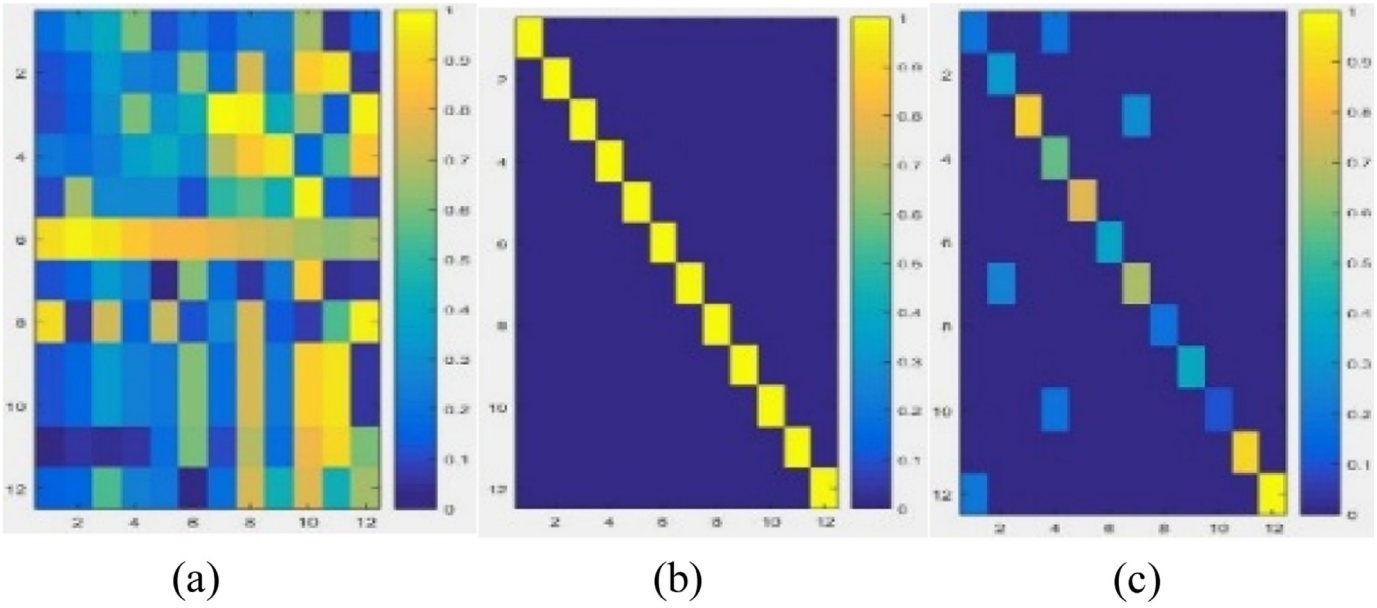

Fig. 6. Log-Whitening Transformation (a) original log-centered covariance matrix (b) whitened covariance matrix (c) log-whitened covariance matrix.

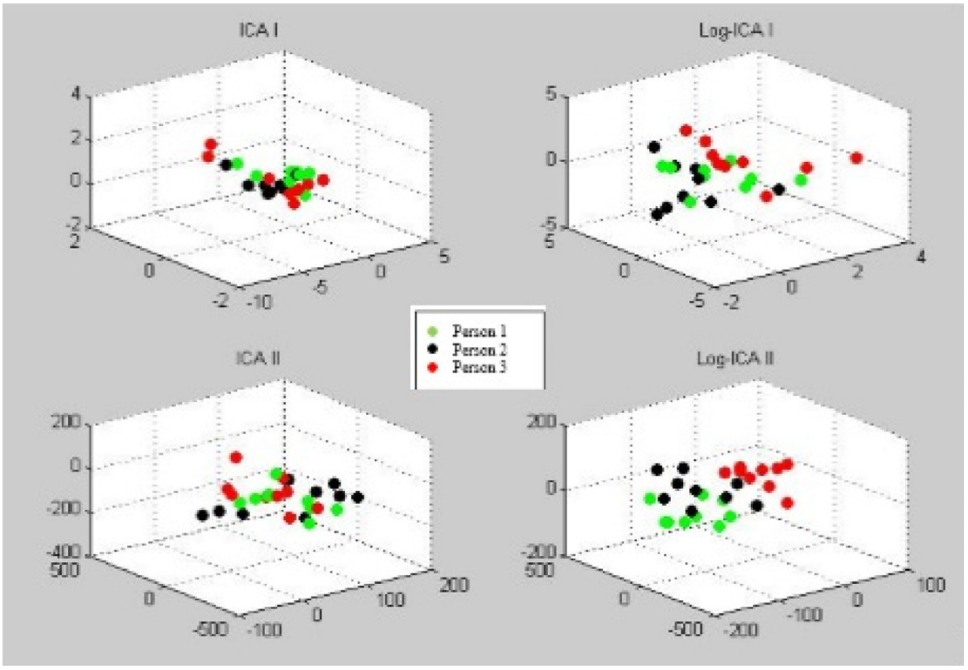

Fig. 7. Three class separation in ICA and Log-ICA.

3.4. Projected feature separation

To illustrate the effectiveness of Log-ICA in class separation, we consider a small subset of the IRIS face dataset to have a simple visualization of separation. We randomly choose three images for each of the three expressions for three arbitrary subjects, a total of 27 face images. An independent subspace is created for these 27 face images, and each of these images is projected into the subspace. The subspace creation and projection of the individual image is shown in Fig. 7 for ICA I, Log-ICA I, ICA II, and Log-ICA II. It is observed that Log-ICA II is more efficient than the ICA I, ICA II, and Log-ICA I to make the three categories separable in projection space.

4. Experimental results and discussions

The present method is evaluated on four distinct tasks: (a) Recognition of visual and thermal face images, (b) Recognition of facial expressions from visual and thermal face images, (c) Face recognition from fused images of thermal and visual face images and (d) Facial expression recognition from fused images of thermal and visual face images. Visual face recognition is evaluated on CMU Pose, Illumination, and Expression (CMU-PIE) database, Facial Recognition Technology (FERET) and YALE face datasets. The IRIS (Imaging, Robotics, and Intelligent Systems) Infrared (IR)/Visible face dataset and USTC-NVIE (Natural Visible and Infrared facial Expression) face datasets are used for visual and thermal face recog-

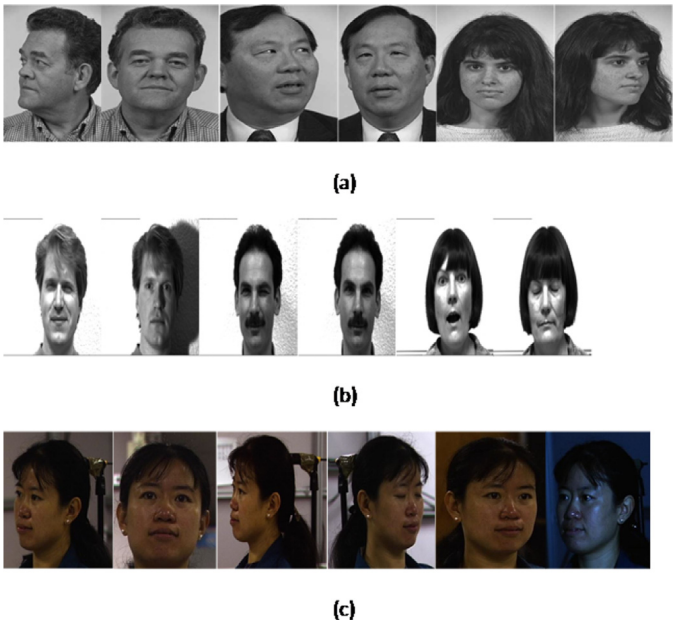

Fig. 8. Sample visual face images of (a) FERET (b) YALE (C) CMU-PIE database.

nition, facial expression recognition and fused face recognition purposes. Visual facial expression recognition experiment is also conducted on Japanese Female Facial Expression (JAFFE) database, Cohn–Kanade AU-Coded Expression Database (CK), and Compound Facial Expressions of Emotion (CFEE) databases.

CMU-PIE dataset (Sim, Baker, & Bsat, 2003) contains 41,368 images of 68 people. The face image of each person is captured under 13 different poses, 43 different illumination conditions, and with four different expressions.

FERET face database (Phillips, Wechsler, Huang, & Rauss, 1998) contains 1564 sets of images for a total of 14,126 images that includes 1199 individuals and 365 duplicate sets of images. A duplicate set is the second set of images of a person already in the database and was usually taken on a different day.

YALE database (Georghiades, Belhumeur, & Kriegman, 2001) comprises 165 GIF images of 15 subjects. There are 11 face images per subject with different expressions or configurations. The sample visual face images of three different databases are shown in Fig. 8.

IRIS Visual/Thermal face database (DOE University Research Program in Robotics, 2005) contains face images of 30 individuals. Total 4228 pairs of IR and visual images are there, and total 176–250 images/person are captured with 11 images per rotation (poses for each expression and each illumination). The subjects are recorded in three different expressions Ex1 (Surprised), Ex2 (laughing), Ex3 (Anger) and mainly five different illuminations with varying poses. In this paper, we consider the expression dataset of total 660 face images with 20 classes and 33 images per class and the illumination dataset of 17 classes with total images of 748 with 44 images per class.

The USTC-NVIE Visual/ Thermal face dataset (Wang et al., 2010) contains only three expressions (surprise, happiness, and anger). Each expression has nine images including three frontal, three oriented toward the left and three right oriented poses. We consider face images without glass only from both visual and infrared datasets. A total number of classes is 30. There are total 270 face images of 30 individuals.

The JAFFE database (Lyons, Akamatsu, Kamachi, & Gyoba, 1998) images are taken at Kyushu University, Japan. Tungsten lights are positioned to create evenly illuminated face images. Ten persons pose themselves for three or four examples of each of the six basic facial expressions, namely, happiness, sadness, surprise, anger, disgust, and fear, along with a neutral face for a total of 219 images of facial expressions.

The CFEE database (Du, Tao, & Martinez, 2014) contains expressive face images of 230 human subjects. Total 21 different expressions were captured. Other than basic, compound expressions were also included in this database.

The CK Database (Kanade, Cohn, & Tian, 2000) includes 486 sequences from 97 posers. Each sequence starts with a neutral expression and continues to a peak expression. The peak expression of each sequence is fully FACS coded and given an emotion label. Subjects perform a series of 23 facial displays that included a single action unit and combinations of action units.

The proposed method is compared to the two architectures of ICA with the combination of five different classifiers. K-Nearest Neighbor (KNN), Support Vector Machine (SVM), Linear Discriminant Analysis (LDA), Decision tree, and Random forest. The face images are manually cropped and resized to 50×50 pixels. For all three kinds of experiments, 10-fold cross-validation is used. The value of K is 7 in the KNN classifier, and SVM classification is conducted with the help of a polynomial kernel with degree 2.

4.1. Face recognition experiment

The visual face recognition experiment is conducted on all five face datasets. The thermal IR face recognition is performed only on two datasets: IRIS and USTC_NVIE face datasets. We conduct the face recognition experiments on five datasets separately. The recognition rates for different face datasets are listed in Table 1.

4.1.1. Face recognition on CMU-PIE datasets

For the task of face recognition, experiments aim to investigate the performance of our method compared to two architectures of ICA using five different classifiers. Here, we choose 300 expressive face images and 1000 illuminated face images of 10 individuals from CMU-PIE dataset. The face images contain different poses. We perform experiments on both expression and illumination datasets separately.

We list the recognition rates of ICA I, ICA II, Log-ICA I and Log-ICA II with five different classifiers in Table 1. The performance measure shows that Log-ICA II with SVM generates a better result than rest other methods in case of expression face dataset. The performance of Log-ICA is worst when it combines with a decision tree.

The performance of SVM is superior to LDA, KNN, and Random Forest with the combination of Log-ICA. Though the recognition rate is too low in illumination dataset, it is noticed that Log-ICA I and Log-ICA II perform better than ICA-I and ICA II. Here, LDA achieves a better result than others. Like the expression dataset, here also decision tree is the worst performer. The reason behind the low recognition rate may be the strong illumination variation in face images, which is not compensated by the Log-ICA algorithm. However, Log-ICA obtains a better result than both architectures of ICA in illumination dataset.

4.1.2. Face recognition on FERET dataset

From the subset of gallery 1196 images, we select entire 539 face images of 34 subjects in our experiment.

The results show that the recognition rate is very low for all classifiers. Besides, Log-ICA II with LDA achieves 59.3% accuracy which is very close to the accuracy of ICA II with LDA (59.23%). Similarly, Log-ICA-I and ICA-I generate almost similar result in combination with LDA. The classification result of SVM is slightly better than the rest three classifiers (KNN, decision tree, and ran-

Table 1
Face recognition rates for different face datasets.

Method	Database	Accuracy (%)											
		Arch-I						Arch-II					
		Non-Logarithm			Logarithm			Non-Logarithm			Logarithm		
		V	T	F	V	T	F	V	T	F	V	T	F
ICA + SVM	CMU-PIE (Exp)	90.66			90.33			95.33			95.89		
	CMU-PIE (Illu)	45.6			49.8			53.2			49.8		
	FERET	44.6			49.6			48.84			48.96		
	YALE	72			76			74.66			74.89		
	IRIS (Exp)	87.66	79.54	88.76	88.18	84.99	90.75	88.17	85.51	88.93	90.51	85.82	90.99
	IRIS (Illu)	96.22	95.71	97.24	96.40	96.41	97.48	96.78	96.81	98.49	96.86	96.94	98.78
	USTC–NVIE	94.44	90.74	95.54	95.92	95.92	96.99	97.4	97.4	97.77	97.4	97.4	98.4
ICA + LDA	CMU-PIE (Exp)	87.33			87.33			86.66			87.33		
	CMU-PIE (Illu)	53			54			53			54		
	FERET	57.69			57.96			59.23			59.3		
	YALE	81.33			81.33			89.33			89.33		
	IRIS (Exp)	88.93	80.75	90.14	90.6	80.93	91.45	89.08	79.99	91.05	90.42	79.99	91.60
	IRIS (Illu)	95.90	94.08	95.95	95.93	95.13	96.01	95.87	94.86	95.98	96.10	94.58	96.45
	USTC–NVIE	98.51	97.4	98.51	98.73	99.62	98.81	98.51	98.14	98.88	98.51	98.14	99.62
ICA + KNN	CMU-PIE (Exp)	59.33			64.66			72			72		
	CMU-PIE (Illu)	28			34.8			36.8			36.8		
	FERET	35			36.08			35.38			35.53		
	YALE	52			70.66			77.33			78.46		
	IRIS (Exp)	79.69	74.54	80.29	80.2	75.14	82.72	83.33	81.51	84.99	83.93	82.27	86.05
	IRIS (Illu)	90.37	90.53	91.07	90.72	90.98	91.25	87.80	91.36	93.55	88.22	92.34	94.45
	USTC–NVIE	90.73	87.03	94.07	88.99	91.81	96.25	89.99	96.29	97.03	91.14	96.59	97.51
ICA + Decision Tree	CMU-PIE (Exp)	36.66			44			45.33			47		
	CMU-PIE (Illu)	17.4			25.8			24.2			26.9		
	FERET	22.3			22.07			22.3			23.53		
	YALE	38.66			46.66			48			57.33		
	IRIS (Exp)	50.3	40.45	50.3	50.3	40.96	50.75	61.36	44.23	56.81	80.73	86.96	91.07
	IRIS (Illu)	61.80	63.96	61.27	60.41	63.58	61.39	56.94	57.42	61.32	56.05	57.47	61.13
	USTC–NVIE	67.51	65.55	67.03	68.51	65.65	69.62	80.73	86.66	89.62	80.73	86.96	91.07
ICA + Random Forest	CMU-PIE (Exp)	63.33			80.66			86			84.66		
	CMU-PIE (Illu)	28.6			33.6			39.8			40.6		
	FERET	38.07			40			41.15			42		
	YALE	53.33			64			72			74.66		
	IRIS (Exp)	79.69	74.54	80.29	80.2	75.14	82.72	93.32	94.81	95.92	83.93	82.27	86.05
	IRIS (Illu)	83.95	89.19	87.67	86.1	90.04	90.65	89.43	94.59	93.95	89.93	94.68	94.72
	USTC–NVIE	86.29	91.47	93.92	85.55	89.62	93.7	93.32	94.81	95.92	94.25	95.36	95.98

dom forest). The accuracy improvement is noticed in Log-ICA II for all the classifiers.

4.1.3. Face recognition on YALE dataset

We consider all 150 face images of 10 subjects where each subject contains 10 face images excluding glass based face images from each subject. The performance shows that the highest accuracy 89.33% is obtained using both ICA II and Log-ICA II with the help of LDA. The performance improves in Log-ICA I and II for the rest other cases. The result of ICA I is highly improved when face images are classified using KNN (18.66% improvement) and Random Forest (10.67% improvement). The classification accuracy of the decision tree is the poorest for both architectures.

It is noticed from the evaluation results of three different databases that the decision tree does not perform well. The reason may be continuous real-valued features of ICA I and ICA II, which are not well suited for decision trees.

4.1.4. Face recognition on IRIS visual/thermal dataset

The database contains the expression dataset, which consists of total 660 face images of 20 persons and the illumination dataset which includes face images of 17 persons with total images of 748. The database comprises both visual and thermal infrared face images. Therefore, we conduct face recognition on both modalities and perform classification on fused face images also. Illumination variation can be compensated using multisensor image fusion technique, which may provide a better recognition rate than a single modality.

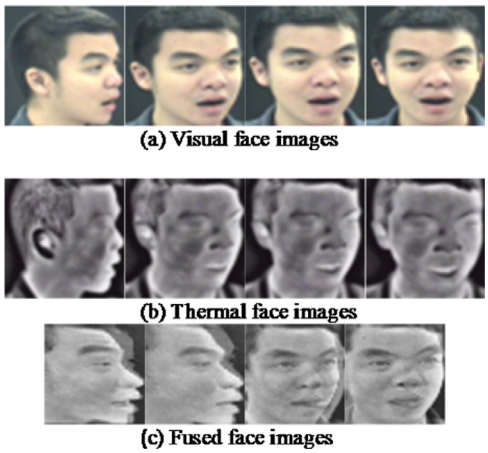

Fig. 9. Sample face images of IRIS database (a) Visual, (b) Thermal, (c) Fused Face Images.

Here, the fusion is carried out based on pixel level fusion scheme where 50% information is taken from the visual face image and rest 50% information comes from the thermal face image. In pixel level fusion, the fusion of pixels can be done by pixel-wise weighted summation of visual and infrared (IR) images. Fig. 9 presents some sample face images of IRIS face database as well

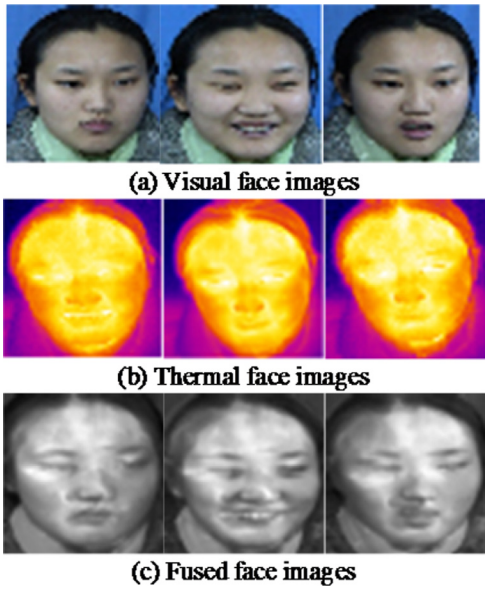

Fig. 10. Sample face images of USTC-NVIE database (a) Visual, (b) Thermal, (c) Fused Face Images.

as fused face images of the corresponding visual and thermal face images.

The fused face image recognition rates, tabulated in Table 1, clearly indicate better recognition rate than individual face recognition performance. The Log-ICA I with LDA achieves the highest accuracy (90.6%) for visual face recognition, and Log-ICA II with SVM obtains 85.82% maximum accuracy for thermal face recognition. However, Log-ICA II with LDA generates maximum accuracy (91.6%) for fused face images where corresponding visual and thermal face recognition rate is 90.42% and 79.99% respectively. We conduct visual, thermal as well as fused face recognition to ensure the effectiveness of Log-ICA over ICA in both architectures. The thermal face recognition results indicate that Log-ICA can handle face images of other modalities also.

4.1.5. Face recognition on USTC-NVIE face dataset

We consider without glass based face images from both visual and infrared modality. The total number of subjects is 30. There are total 270 face images of 30 individuals. The visual, thermal and corresponding fused face images are shown in Fig. 10.

Observations reveal that the highest accuracy is obtained through Log-ICA II and LDA in all three cases. The classification accuracy of ICA II and LDA is almost similar to Log-ICA II and LDA. The recognition rate of fused face images is better than individual modalities. One interesting observation is noticed here that the recognition rate for thermal face images is higher than the recognition rate for visual face images in most of the cases.

4.2. Facial expression recognition experiment

The expression recognition experiments are conducted on five different facial expression datasets namely IRIS visual/thermal face database, USTC-NVIE face dataset, Cohn-Kanade (CK), Compound Facial Expressions of Emotion (CFEE) and Japanese Female Facial Expression (JAFFE) database. First two datasets are already introduced earlier, and five expressive face images from each of the three newly included face datasets are shown in Fig. 11. In our experiment, we consider all six basic expressions namely anger, disgust, fear, happy, surprise and sad. The facial expression recognition accuracies for all five databases are listed in Table 2.

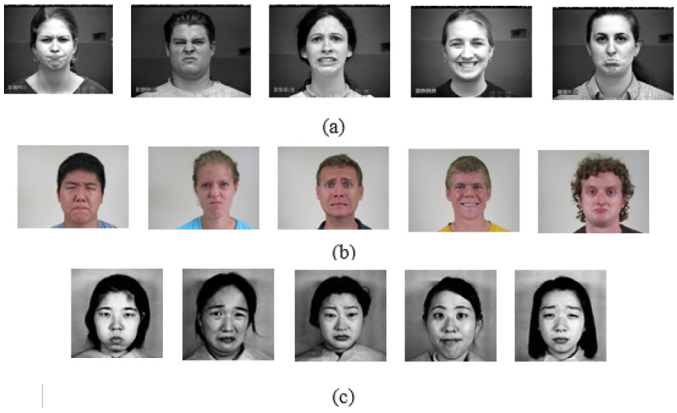

Fig. 11. Sample visual expressive face images of (a) CK (b) CFEE (c) JAFFE database.

4.2.1. Facial expression recognition on CK dataset

We randomly select facial expressions of different persons. Experiment results indicate that Log-ICA I is not effective for recognizing expressions in comparison to Log-ICA II. Though the expression recognition rate is low enough, accuracy improves noticeably in the case of Log-ICA II extracted features. The performance of Log-ICA II is lower than ICA II when combined with LDA. The performance improvement is noticed in Log-ICA II in combination with the classifiers SVM, KNN, Decision Tree, and Random Forest. The maximum accuracy (49.81%) is attained through Log-ICA II and SVM in this database.

4.2.2. Facial expression recognition on JAFFE dataset

We consider frontal expressive face images of ten subjects for our experiment. From the Table 2, it is evident that like the previous one, here also Log-ICA I does not make any improvement over ICA I. The accuracy of Log-ICA II is almost similar to ICA II in combination with SVM and LDA. ICA II with SVM achieves only 0.84% higher accuracy than Log-ICA II, and this recognition rate is the highest rate for this dataset. Huge performance improvement (more than 23%) is observed in the combination of Log-ICA II and Random Forest in comparison to ICA II. Decision tree also performs better for Log-ICA II than ICA II.

4.2.3. Facial expression recognition on CFEE dataset

We choose six basic expressions of 50 subjects from the database. The classifier SVM achieves the highest accuracy for ICA II extracted features. The accuracy of Log-ICA II improves 7.78% and 4.45% for LDA and KNN respectively. The performance of Log-ICA I slightly improves when it combines with LDA and Decision Tree.

4.2.4. Facial expression recognition on IRIS dataset

In the IRIS dataset, each expression contains 11 face images. We perform expression recognition experiment on visual, thermal and fused face images. It is observed from the experiment that fused facial expression recognition rate is lesser than the individual modality expression recognition rate. The overall recognition rate is also meager.

The performance of Log-ICA II is slightly better in the case of fused facial expression recognition than ICA II for all the classifiers except SVM. In combination with SVM and LDA, Log-ICA I shows accuracy improvement than ICA I. The reason behind the too low recognition rates may be the inclusion of pose variations with each expression for each subject in experimental dataset. Pixel level fusion may not be effective enough for expression recognition.

4.2.5. Facial expression recognition on USTC-NVIE dataset

We select 360 face images for 20 subjects in our experiment. Each expression has three face images. In this database also, Log-

Table 2
Facial expression recognition rates for different face datasets.

Method	Database	Accuracy (%)											
		Arch-I						Arch-II					
		Non-Logarithm			Logarithm			Non-Logarithm			Logarithm		
		V	T	F	V	T	F	V	T	F	V	T	F
ICA + SVM	CK	31.90			31.90			43.39			49.81		
	CFEE	52.38			51.95			64.55			63.44		
	JAFFE	64.16			64.16			78.5			77.66		
	IRIS	24.6	21.9	17.63	22.6	21.7	17.8	16.38	20.27	16.94	16.38	18.61	16.38
	USTC-NVIE	20.83	27.5	26.25	20.41	22.91	24.16	48.38	52.41	60.91	41.66	54.83	51.66
ICA + LDA	CK	22.85			22.85			45.28			39.62		
	CFEE	41.42			42.38			53.33			61.11		
	JAFFE	45			44.16			76.66			75		
	IRIS	23.33	25	18	28.66	23	21.33	17	22	20	22	26	21
	USTC-NVIE	20.41	21.66	24.16	17.91	21.25	19.58	40.83	41.66	49.16	31.66	40	40.83
ICA + KNN	CK	22.85			22.85			33.96			43.39		
	CFEE	41.42			41.42			46.66			51.11		
	JAFFE	42.5			41.66			56.66			46.66		
	IRIS	20.66	23	21.66	19.66	16.66	17	19.33	17.33	14	20.33	17.66	16.66
	USTC-NVIE	22.5	15.41	22.5	19.58	15	22.08	46.66	35	45	45	35	37.5
ICA + Decision Tree	CK	13.14			11.52			21.13			31.50		
	CFEE	21.09			21.38			31.77			30.11		
	JAFFE	23			22.33			24.66			39.16		
	IRIS	27.83	28.5	27.63	23	21.66	21.23	21.93	20.4	17.23	22.7	23.46	20.46
	USTC-NVIE	13.58	15.87	16.25	13.29	15.70	13.54	24.33	30	24.91	25.83	32.08	27
ICA + Random Forest	CK	23.32			22.66			29.62			43.01		
	CFEE	31.90			31.57			44.38			44.11		
	JAFFE	34			33.25			40.5			63.16		
	IRIS	20.4	24.06	19.96	12.93	15.6	12.63	13.2	13.46	12.06	14	14.93	12.46
	USTC-NVIE	20.41	21.66	24.16	17.91	21.25	19.58	40.83	41.66	49.16	31.66	40	40.83

ICA does not become efficient enough to improve the performance of ICA. The maximum accuracy (60.91%) is achieved through ICA II with SVM in recognizing fused facial expressions. Except ICA II combined with SVM and LDA, it is noticed that fused facial expression recognition rate is higher than visual one but lower than thermal. The high accuracy in thermal facial expression recognition indicates that thermal face image contains more informative features than visual one and as a result, fused images add important thermal features in it resulting in higher recognition rate than visual facial expressions.

From the experimental results, we can say that noticeable performance improvement occurs using Log-ICA II in case of expression recognition. Therefore, we consider facial expression as a multiplicative noise of face image, which is converted into additive noise using Logarithmic transform. We describe the association between facial expression and multiplicative noise in Appendix.

4.3. Noisy visual face recognition experiment

The robustness of our proposed approach is ensured with the recognition of noisy face images. Three noise types are induced in our visual face image datasets, which are Gaussian noise, impulse noise, and multiplicative noise. The experiment is conducted for a noise variance of 0.04 (applicable for Gaussian and multiplicative noise). In the case of impulse noise, the noise density is 0.04. From the previous recognition results, it is noticed that Log-ICA II performs better than Log-ICA I. In this experiment, we consider only Log-ICA II for noisy face image recognition. Accuracy improvement is noticed in Log-ICA II for all face datasets except IRIS (Illum) in Table 3. Accuracy is improved for all three types of noises.

Table 3
Facial recognition rates for different face datasets in noise.

Noise	Database	Accuracy	
		ICA II	Log-ICA II
Gaussian (Additive)	USTC-NVIE	94.44	96.66
	FERET	45	45.38
	YALE	74.66	78.66
	CMU-PIE (Exp)	87.33	90
	CMU-PIE (Illum)	43.2	46
	IRIS (Exp)	85.30	90.90
	IRIS (Illum)	95.58	94.35
Salt&Paper	USTC-NVIE	94.44	95.55
	FERET	44.23	48.84
	YALE	73.33	77.33
	CMU-PIE (Exp)	87.33	92
	CMU-PIE (Illum)	46.2	52
	IRIS (Exp)	86.51	89.09
	IRIS (Illum)	95.96	95.58
Speckle (Multiplicative)	USTC-NVIE	94	96.66
	FERET	44.61	45.76
	YALE	66.66	76
	CMU-PIE (Exp)	88.66	92.66
	CMU-PIE (Illum)	41.4	46.8
	IRIS (Exp)	88.18	89.54
	IRIS (Illum)	96.36	95.88

4.4. Comparative study

We compare our proposed method Log-ICA with two enhanced versions of ICA. As we conduct experiments on five different face datasets, we only consider one face dataset, i.e., Yale face dataset for comparison purpose. The comparative study in Table 4 shows that Log-ICA II performs better than previous ICA based algorithms (EICA and BICA).

5. Conclusion and future work

An approach to face recognition using natural Logarithm based Independent Component Analysis (Log-ICA) is presented here. We demonstrate the efficiency of our approach on different face datasets, which contains images gathered with varying lighting, facial expression, pose. In this paper, human face images of varying expressions are also recognized using five different classifiers.

Table 4
Comparative study.

Method	Face Recognition Accuracy (Yale Face dataset)
EICA (Liu, 2004)	68.89%
BICA (Zhang et al., 2007)	75.56%
ICA I + KNN	52%
ICA II + KNN	77.33%
Log-ICA I + KNN	70.66%
Log-ICA II + KNN	78.46%

We highlight the enhanced result of Log-ICA II in combination with different classifiers, which is comprehended through the accuracy rate. The proposed method is robust enough in recognizing noisy face images. The overall expression recognition rate is low for both ICA and Log-ICA. However, noticeable improvement is seen in Log-ICA II in recognizing expressions that ensures that Log-ICA II is suitable enough for expression recognition. In the future, it would be interesting to work with complicated face datasets like low resolution and occluded face images.

Credit author statement

Mrinal Kanti Bhowmik- Conceptualization, Methodology, Project Administration, Funding Acquisition, Resources.

Priya Saha- Formal Analysis, Writing – Original Draft, Writing – Review & Editing, Visualization, Funding Acquisition.

Anu Singha- Software, Validation, Formal Analysis, Investigation, Data Curation, Visualization.

Debotosh Bhattacharjee- Writing – Review & Editing, Visualization, Supervision.

Paramartha Dutta- Writing – Review & Editing, Visualization, Supervision.

Acknowledgment

The second author is grateful to the Department of Science and Technology (DST), Government of India for providing her Junior Research Fellowship-Professional (JRF-Professional) under DST-INSPIRE fellowship program(No. IF131067).

Appendix

Representation of facial expression as multiplicative noise

Facial expression can be expressed using the parameters of an Active Appearance Model (AAM). AAM represents displacements from the origin in the space spanned by the model. If we multiply the parameters by a scalar greater than unity, the distance from the mean is increased. Therefore, facial expression can be mapped and manipulated using the AAM parameters and expressed as (8).

$$S = S_0 + \sum_{i=1}^{m} S_i P_i \alpha \tag{8}$$

The shape S is defined as the concatenation of the x and y coordinates of n landmark points of the face image.

$S = (x_1, y_1, x_2, y_2, \ldots, x_n, y_n)^T$ and $P = (p_1, p_2, \ldots, p_n)^T$ is the shape parameter vector that represents expression variations. The base shape S_0 is the mean shape and the vectors S_i are the reshaped Eigenvectors corresponding to the m largest Eigenvalues.

Now if we apply natural logarithm operator on both sides of (8), it becomes

$$\log(S) = \log\left(S_0 + \sum_{i=1}^{m} S_i P_{i\alpha}\right)$$
$$\log(S) = \log(S_0 + B)$$
$$\log(S) = \log(S_0) + \log(B/S_0 + 1)$$
$$\log(S) = \log(S_0) + \log(B_1 + 1)$$
$$\log(S) = \log(S_0) + \log(B_2) \tag{9}$$

We can say from (8) that the vector B_2 comprises principal components of an expressive face image which may be the important features responsible for generating facial expressions. This means that when these important features are appended with the neutral face image, the face becomes expressive.

Multiplicative noise is represented by multiplication of original image u and noise n. The recorded image g can be written by

$$g = u \times n \tag{10}$$

Here, u, g and n are $n^2 \times 1$ vector corresponding to $n \times n$ image. If we apply natural logarithm operator on both sides of (10), we get

$$\log(g) = \log(u) + \log(n) \tag{11}$$

By comparing (9) and (11), we can say that expressive facial features can be taken as a multiplicative noise for face images. Therefore, when faces are expressive, recognition of those face images becomes difficult. The face images with expression, which are also considered as multiplicative noise over neutral face images, become easier to handle as logarithmic transformation converts a multiplicative noise into an additive noise.

References

Bach, F. R., & Jordan, M. I. (2002). Kernel independent component analysis. *Journal of Machine Learning Research, 3*, 1–48.

Bartlett, M. S., Movellan, J. R., & Sejnowski, T. J. (2002). Face recognition by independent component analysis. *IEEE Transactions on Neural Networks, 13*(6), 1450–1464.

Belhumeur, P., Hespanha, J., & Kriegman, D. (1997). Eigenfaces vs. fisherfaces: Recognition using class specific linear projection. *IEEE Transactions on Pattern Analysis and Machine Intelligence, 19*(7), 711–720.

Beveridge, J. R., Zhang, H., Draper, B. A., Flynn, P. J., Feng, Z., Huber, P., et al. (2015). Report on the FG 2015 video person recognition evaluation. *2015 11th IEEE international conference and workshops on automatic face and gesture recognition (FG)*.

Bhowmik, M. K., Bhattacharjee, D., Basu, D. K., & Nasipuri, M. (2011). Facial expression invariant person recognition using feature level fusion of visual and thermal images. *2011 world congress on information and communication technologies*.

Bhowmik, M. K., Bhattacharjee, D., Basu, D. K., & Nasipuri, M. (2012). Eye region-based fusion technique of thermal and dark visual images for human face recognition. *Optical Engineering, 51*(7), 077205.

Choi, J. Y., Neve, W. D., Plataniotis, K. N., & Ro, Y. M. (2011). Collaborative face recognition for improved face annotation in personal photo collections shared on online social networks. *IEEE Transactions on Multimedia, 13*(1), 14–28.

Comon, P. (1994). Independent component analysis, a new concept? *Signal Processing, 36*(3), 287–314.

Ding, C., & Tao, D. (2015). Robust face recognition via multimodal deep face representation. *IEEE Transactions on Multimedia, 17*(11), 2049–2058.

Du, S., Tao, Y., & Martinez, A. M. (2014). Compound facial expressions of emotion. *Proceedings of the National Academy of Sciences, 111*(15), E1454–E1462.

Georghiades, A., Belhumeur, P., & Kriegman, D. (2001). From few to many: Illumination cone models for face recognition under variable lighting and pose. *IEEE Transactions on Pattern Analysis and Machine Intelligence, 23*(6), 643–660.

Han, H., Otto, C., Liu, X., & Jain, A. K. (2015). Demographic estimation from face images: Human vs. machine performance. *IEEE Transactions on Pattern Analysis and Machine Intelligence, 37*(6), 1148–1161.

Hsieh, C.-K., Lai, S.-H., & Chen, Y.-C. (2009). Expression-invariant face recognition with constrained optical flow warping. *IEEE Transactions on Multimedia, 11*(4), 600–610.

DOE University Research Program in Robotics, 2005. https://www.cse.ohio-state.edu/otcbvsbench/Data/02/download.html

Hyvarinen, A. (1999). Fast and robust fixed-point algorithms for independent component analysis. *IEEE Transactions on Neural Networks, 10*(3), 626–634.

Hyvärinen, A., Karhunen, J., & Oja, E. (2002). ICA by maximization of nongaussianity. In S. Haykin (Ed.), *Independent component analysis* (pp. 165–202). New York: John Wiley & Sons Inc.

Kanade, T., Cohn, J., & Tian, Y. (2000). Comprehensive database for facial expression analysis. In *Proceedings fourth IEEE international conference on automatic face and gesture recognition (Cat. No. PR00580)*.

Lee, T.-W., Girolami, M., & Sejnowski, T. J. (1999). Independent component analysis using an extended infomax algorithm for mixed subgaussian and supergaussian sources. *Neural Computation, 11*(2), 417–441.

Liu, C. (2004). Enhanced independent component analysis and its application to content based face image retrieval. *IEEE Transactions on Systems, Man and Cybernetics, Part B (Cybernetics), 34*(2), 1117–1127.
Lyons, M., Akamatsu, S., Kamachi, M., & Gyoba, J. (1998). Coding facial expressions with Gabor wavelets. In *Proceedings third IEEE international conference on automatic face and gesture recognition*.
Phillips, P., Martin, A., Wilson, C., & Przybocki, M. (2000). An introduction evaluating biometric systems. *Computer, 33*(2), 56–63.
Phillips, P., Wechsler, H., Huang, J., & Rauss, P. J. (1998). The FERET database and evaluation procedure for face-recognition algorithms. *Image and Vision Computing, 16*(5), 295–306.
Stone, J. V. (2004). *Independent component analysis: a tutorial introduction*. Cambridge: MIT Press.
Sim, T., Baker, S., & Bsat, M. (2003). The CMU pose, illumination, and expression database. *IEEE Transactions on Pattern Analysis and Machine Intelligence, 25*(12), 1615–1618.
Wang, S., Liu, Z., Lv, S., Lv, Y., Wu, G., Peng, P., et al. (2010). A natural visible and infrared facial expression database for expression recognition and emotion inference. *IEEE Transactions on Multimedia, 12*(7), 682–691.
Whittaker, E. T., & Watson, G. N. (1990). *A course in modern analysis* (4th ed.). Cambridge, England: Cambridge University Press.
Yin, X., & Liu, X. (2018). Multi-task convolutional neural network for pose-invariant face recognition. *IEEE Transactions on Image Processing, 27*(2), 964–975.
Zen, G., Porzi, L., Sangineto, E., Ricci, E., & Sebe, N. (2016). Learning personalized models for facial expression analysis and gesture recognition. *IEEE Transactions on Multimedia, 18*(4), 775–788.
Zhang, L., Gao, Q., & Zhang, D. (2007). Block independent component analysis for face recognition. *14th international conference on image analysis and processing (ICIAP 2007)*.